

## SUPPLEMENTARY INFORMATION

## Strain-Induced Deformation of Glassy Spherical Microdomains in Elastomeric Triblock

## Copolymer Films:

## Simultaneous Measurements of a Stress-Strain Curve with 2d-SAXS Patterns

Shogo Tomita<sup>1</sup>, Li Lei<sup>2</sup>, Yoshimasa Urushihara<sup>2</sup>, Shigeo Kuwamoto<sup>2</sup>, Tadashi Matsushita<sup>3</sup>, Naoki Sakamoto<sup>3</sup>, Sono Sasaki<sup>1</sup>, and Shinichi Sakurai<sup>1,\*</sup>

<sup>1</sup>Department of Biobased Materials Science, Kyoto Institute of Technology,  
Matsugasaki, Sakyo-ku, Kyoto 606-8585, Japan

<sup>2</sup> Synchrotron Radiation Nanotechnology Laboratory, University of Hyogo, Tatsuno,  
Hyogo 679-5165, Japan

<sup>3</sup>Asahi Kasei Corporation, 1-105 Kanda Jinbocho, Chiyoda-ku, Tokyo 101-8101, Japan

\*To whom all correspondence should be addressed.

E-mail: shin@kit.ac.jp

Tel: +81-75-724-7864

Fax: +81-75-724-7547

keywords

block copolymer, thermoplastic elastomer, small-angle X-ray scattering, uniaxial stretching, spherical microdomain, prolate-shape microdomain

In this supporting information, we show (1) original stress-strain curves obtained by the simultaneous measurements with 2d-SAXS, (2) the sector averaging method with an anomalous sector range to obtain the 1d-SAXS profile from the 2d-SAXS pattern, (3) the method to determine the peak position of (110) reflection in  $q$  direction parallel to SD from the 2d-SAXS pattern, (4) examples of size distributions used for the model calculation of the 1d-SAXS profiles, and (5) examples of orientational distribution,  $\Psi(\phi)$ , used for the model calculation of the 1d-SAXS profiles in the unloading process.

### **(1) Original stress-strain curves obtained by the simultaneous measurements with 2d-SAXS**

We showed the results of stress measurements as a function of  $(d-d_0)/d_0$  in the main text in Fig. 2. In this Supplementary Information, the original SS curves directly obtained by the simultaneous measurements with 2d-SAXS are shown in Fig. S1 based on which the results shown in Fig. 2 were obtained.

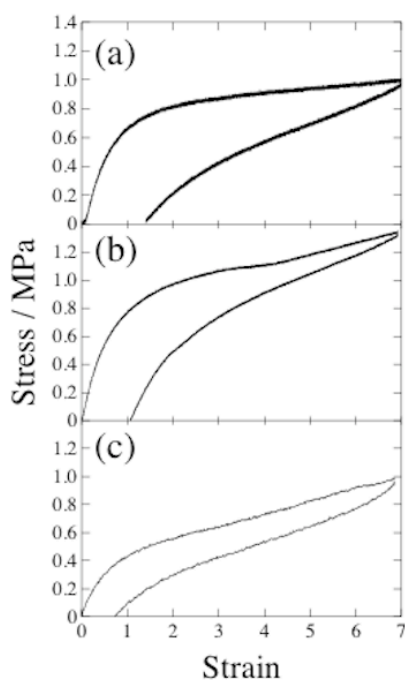


Figure S1 SS curves measured for the (a) SEBS-8, (b) SEBS-16 and (c) SIBS specimens. These are the results by simultaneous measurements with 2d-SAXS.

**(2) The sector averaging method with an anomalous sector range to obtain the 1d-SAXS profile from the 2d-SAXS pattern**

Upon stretching, the round-shaped lattice peaks deform as shown in Figs. 3-5. From such deformed 2d-SAXS pattern, sector-averaging to obtain the 1d-SAXS profile in the  $q$  direction parallel to SD does not cause a big problem because the choice of sector angle for the sector-averaging does not sensitively affect the resulted 1d-SAXS profile. On the other hand, a very narrow range of sector angle must be chosen for the  $q$  direction perpendicular to SD. Otherwise, the peak width of the (110) reflection in the resulted 1d-SAXS profile becomes large (smeared) due to the elliptic shape of the (110) reflection. However, the peak of particle scattering becomes obscure when the range of sector angle is too narrow. To increase the intensity of the particle scattering,

a wider range of sector angle is required. Thus, the requirements for the range of the sector angle are contradictory. To fulfill both requirements, we adopted an anomalously designated sector-area as schematically shown with yellow in the 2d-SAXS pattern measured for SEBS-16 at strain of 2.52 as an example (Fig. S2). Here, the sector angle is  $0.5^\circ$  for  $0 < q < 0.66 \text{ nm}^{-1}$  and  $20^\circ$  for  $q \geq 0.66 \text{ nm}^{-1}$ . Consequently, we obtained 1d-SAXS profiles as shown in the panel (b) of Figs. 6-8.

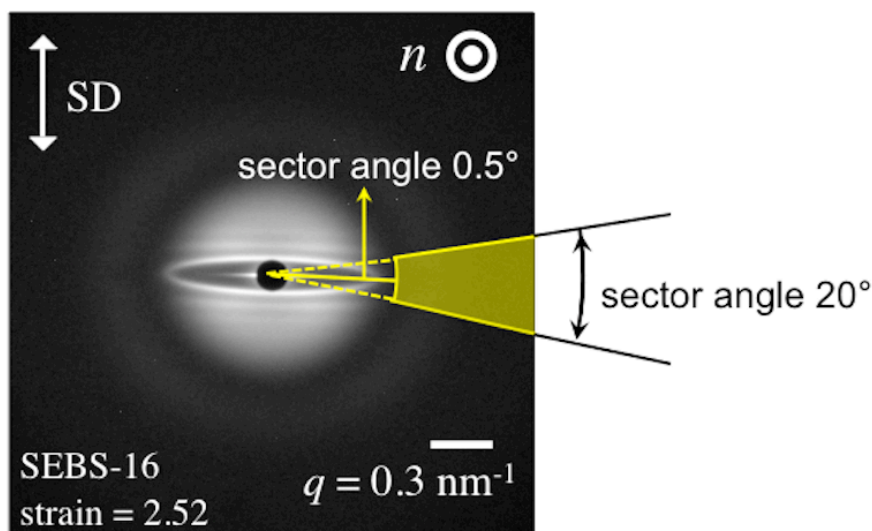


Figure S2 Schematic expression of an anomalously designated sector area, which is shown with yellow in 2d-SAXS pattern measured for SEBS-16 at strain of 2.52, as an example, for conducting the sector-averaging of a 2d-SAXS pattern. Note that sector angle is  $0.5^\circ$  for  $0 < q < 0.66 \text{ nm}^{-1}$  and  $20^\circ$  for  $q \geq 0.66 \text{ nm}^{-1}$ .

### (3) The method to determine the peak position of (110) reflection in $q$ direction parallel to SD from the 2d-SAXS pattern

Since the deformed peak of the (110) reflection was blocked by the beam stopper in  $q$  direction parallel to SD, it is not possible to determine the peak position in

the 1d-SAXS profiles (see panel (a) of Figs. 6-8). Therefore, it is required to determine the peak position directly from the 2d-SAXS pattern. For this purpose, we adopted a method as shown in Fig. S3. Note that the ellipse shown by the broken curve is drawn so as to trace the deformed peak of the (110) reflection. For this purpose, we used the relationship between the azimuthal angle ( $\omega$ ) and the deformation ratio ( $d/d_0$ ) as expressed by eq. S1 in the literature<sup>1</sup>.

$$d/d_0 = \left[ \alpha_x^2 \cos^2 \omega + (1/\alpha_x) \sin^2 \omega \right]^{1/2} \quad (\text{S1})$$

Here,  $\alpha_x$  designates the mechanical stretching ratio of the specimen,  $d$  denotes  $d$ -spacing of the (110) planes perpendicular to the direction which inclines from the equator with the angle of  $\omega$ , and  $d_0$  does  $d$ -spacing of the (110) planes before stretching. Then, the peak position in  $\mathbf{q}_{//}$  was estimated from the minor radius of the ellipse.

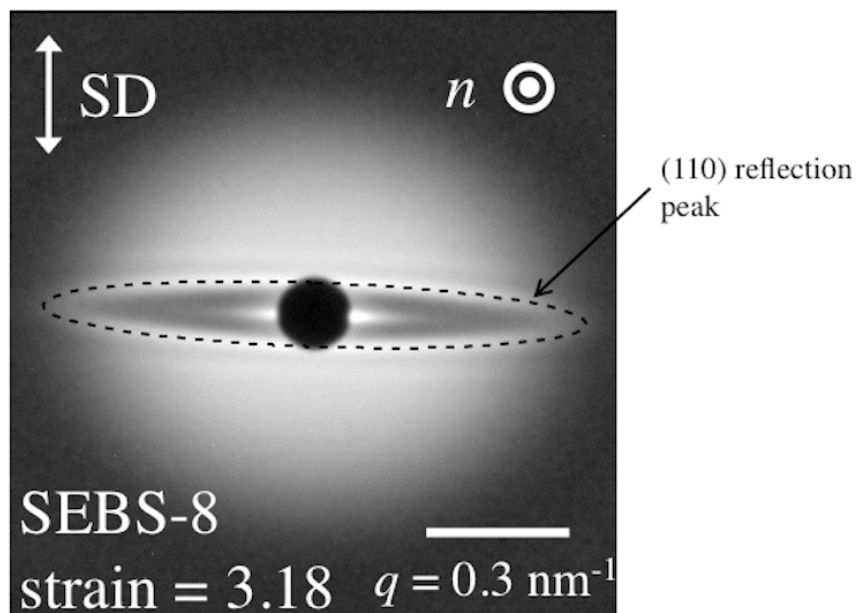


Fig. S3 Schematic expression of the method to determine the peak position of the (110) reflection in  $q$  direction parallel to SD, which is blocked by the beam stopper as shown in the 2d-SAXS pattern for SEBS-8 obtained at strain of 3.18, as an example. Note that the ellipse shown by the broken curve is drawn so as to trace the deformed peak of the (110) reflection.

#### (4) Examples of size distributions used for the model calculation of the 1d-SAXS profiles

To discuss quantitatively shifts of the particle scattering peaks in the stretching process, we attempted to reproduce the 1d-SAXS profiles with model calculation of prolate spheroids. First,  $\Xi(R_{\min})$  was determined to obtain the results of model calculation of 1d-SAXS profile in the  $q_{\perp}$  direction using Gauss function. And then  $\Omega(v)$  was determined from the 1d-SAXS profiles in the  $q_{\parallel}$  direction. In Fig. S4, examples of distributions used for the model calculation of the 1d-SAXS profiles are shown. Panel (a) shows  $\Xi(R)$  at strain of 0 and  $\Xi(R_{\min})$  at strain of 3.18 for SEBS-8, panel (b) shows  $\Omega(n)$  at strain of 3.18 for SEBS-8, panel (c) shows  $\Xi(R)$  at strain of 0

and  $\Xi(R_{\min})$  at strain of 2.31 for SEBS-16, and panel (d) shows  $\Omega(n)$  at strain of 2.31 for SEBS-16.

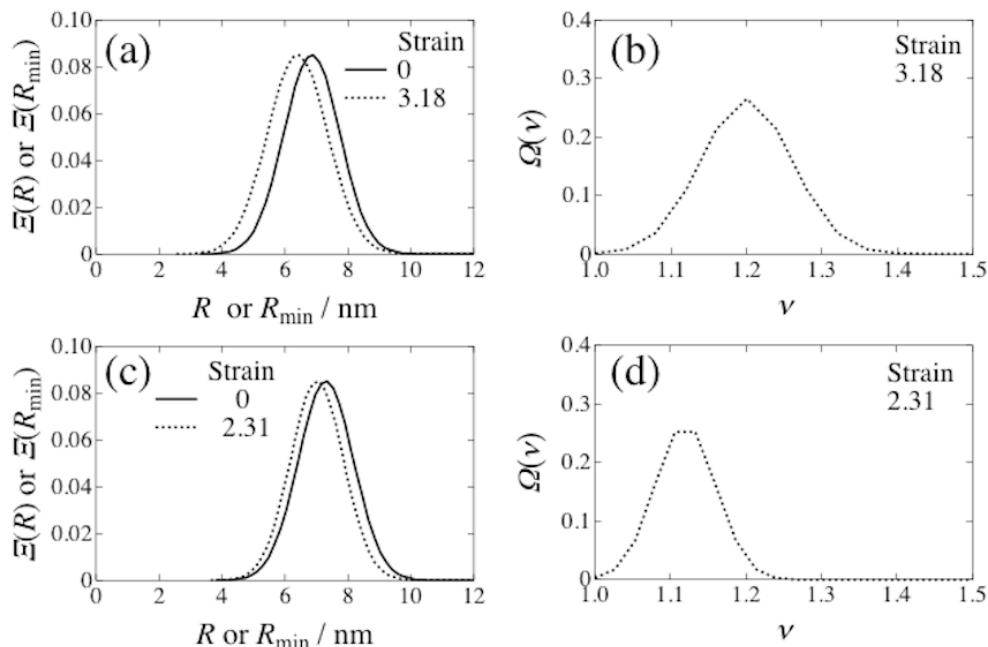


Figure S4 Examples of size distributions used for the model calculation of the 1d-SAXS profiles. (a)  $\Xi(R)$  at strain of 0 and  $\Xi(R_{\min})$  at strain of 3.18 for SEBS-8, (b)  $\Omega(v)$  at strain of 3.18 for SEBS-8, (c)  $\Xi(R)$  at strain of 0 and  $\Xi(R_{\min})$  at strain of 2.31 for SEBS-16, (d)  $\Omega(v)$  at strain of 2.31 for SEBS-16.

#### (5) Examples of orientational distribution, $\Psi(\phi)$ , used for the model calculation of the 1d-SAXS profiles in the unloading process

To understand the behavior of the particle scattering peaks upon unloading, we assumed that plastically deformed PS domains can never recover spherical shape but the perfect orientation of prolate spheroids is relaxed. Here, we set the Gauss function for  $\Psi(\phi)$ , while  $\Omega(v)$  and  $\Xi(R_{\min})$  are fixed with the values obtained for the specimen at maximum strain. Fig. S5 shows examples of orientational distribution,  $\Psi(\phi)$ , used for the model calculation of the 1d-SAXS profiles in the unloading process for (a) SEBS-8

and (b) SEBS-16. It is clearly seen in Fig. S5 that the orientational relaxation of prolate spheroids proceeded in the unloading process. From  $\Psi(\phi)$ , the second-order orientation factor,  $F$ , can be evaluated.

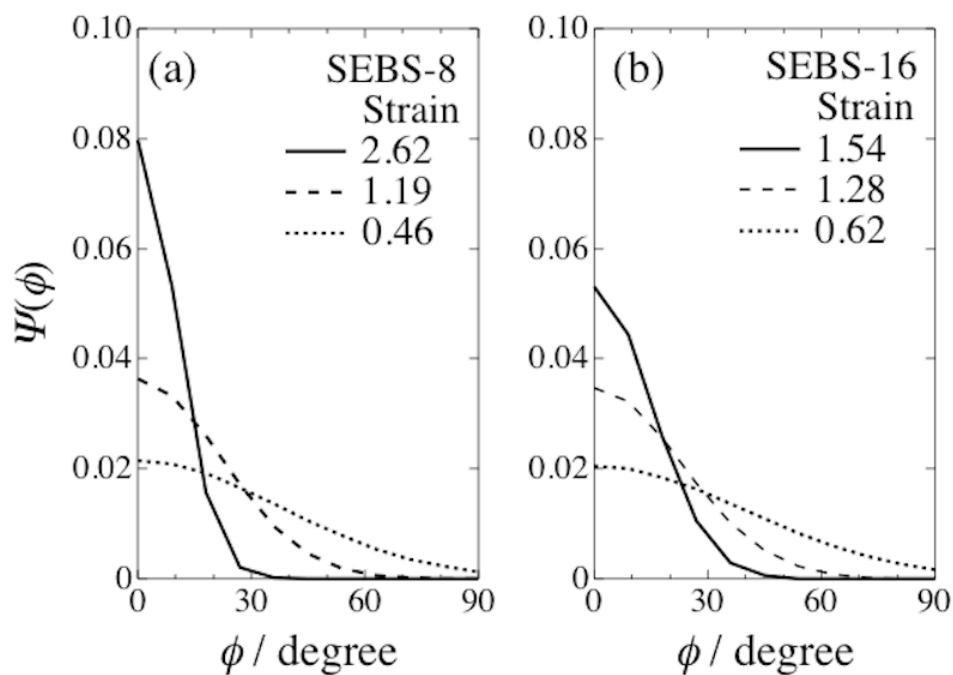


Figure S5 Examples of orientational distribution,  $\Psi(\phi)$ , used for the model calculation of the 1d-SAXS profiles in the unloading process for (a) SEBS-8 and (b) SEBS-16.

### Reference

1. Seguela, R.; Prudhomme, J. Affinity of Grain Deformation in Mesomorphic Block Polymers Submitted to Simple Elongation. *Macromolecules* **1988**, 21, 635-643.